BioMACROMOLECULES

Rapid Polymer Conjugation Strategies for the Generation of pH-Responsive, Cancer Targeting, Polymeric Nanoparticles

Weishuo Li, Jin Geng, Helen Titmarsh, Alicia Megia-Fernandez, Kev Dhaliwal, Margaret Frame, and Mark Bradley

Just Accepted

ACS Publications

Rapid Polymer Conjugation Strategies for the Generation of pH-Responsive, Cancer Targeting, Polymeric Nanoparticles

Weishuo Li,[†] Jin Geng,*[†] Helen Titmarsh,[‡,§] Alicia Megia-Fernandez,[†] Kev Dhaliwal,[‡] Margaret Frame,[§] Mark Bradley*[†]

[†] School of Chemistry, University of Edinburgh, Edinburgh, UK

[‡] The MRC Centre for Inflammation Research, Queen's Medical Research Institute, University of Edinburgh, Edinburgh, UK

[§] Edinburgh Cancer Research UK Centre, Institute of Genetics and Molecular Medicine, University of Edinburgh, Western General Hospital, Crewe Road South, Edinburgh, UK

ABSTRACT

The combination of controlled living polymerization in association with rapid and highly efficient macromolecule conjugation strategies provides a powerful tool for the synthesis of novel polymeric materials. Here functional block copolymers were rapidly and quantitatively conjugated using an efficient reaction between polymers containing a phenolic group and the 4-phenyl-3H-1,2,4-triazole-3,5(4H)-dione (PTAD) moiety, and used to generate nanoparticles that

encapsulated drugs. This rapidly growing field in nanotechnology for biomedical applications provides opportunities to design and develop multifunctional devices that can target, diagnose, controlled delivery of drugs, and treat cancer more efficiently. Here pH responsive amphiphilic block copolymers, which self-assemble into nanoparticles, were fabricated using our novel polymer conjugation strategy with the resulting system designed to promote drug release within the acidic milieu of the cancer microenvironment. The conjugation strategy also enabled the direct tagging of the nanoparticles with a range of fluorophores and/or targeting assets, with cargo release demonstrated in cancer cells.

INTRODUCTION

Nanomedicine requires efficient nanoparticle synthesis, cellular targeting and controlled drug release, and driven by this need a number of micelle systems have been successfully developed. This includes stimuli responsive nanomaterials, with triggers ranging from small molecules,[1] heat, magnetic fields, ultrasound, pH and light, sometimes referred to as "smart", or "environmentally-sensitive" materials.[2-4] The functional requirements needed for effective nanoparticle drug delivery are multitude and include circulatory stability, target localization, cellular binding and/or entry, endosomal escape, and of course controlled drug release. The precise, and multifunctional, combination of these features in one delivery system is challenging.[2,5]

The development of such systems is currently heavily reliant on responsive polymeric materials and over the past two decades, numerous self-assembling nanostructures of amphiphilic block copolymers have been utilized as nanocarriers[6] of drugs,[7] nucleic acids,[8-10] and imaging/contrast agents.[11,12] Often these carry poorly water-soluble drugs, promoting

bioavailability and avoiding rapid liver and urinary clearance. Typically two approaches are used to prepare block copolymers with well-defined structures. [11,13] One is to polymerize a series of monomers sequentially through controlled polymerization techniques (such as ionic or "living" radical polymerization), and the other is to conjugate different polymers. [14,15] Since block copolymers with desired monomer composition are often chemically incompatible, polymer conjugation is often the method of choice. [16,17]

For polymer conjugation chemistries, there is a growing attraction in the polymer community to the employment of reactions, such as azide-alkyne, [18] 'thiol-ene', [19] RAFT-hetero Diels-Alder cycloaddition (RAFT-HAD), [20] or tetrazine-norbornene reactions [21] to conjugate polymeric components, however, each has its limitations, [18] with reactions in aqueous environments (needed for many nanoparticles) often challenging. Recently, cyclic diazodicarboxamides (4-phenyl-3H-1,2,4-triazole-3,5(4H)-dione (PTAD)) have been introduced as a reagent that reacts selectively with the side chain of tyrosine through Friedel-Crafts type chemistry in aqueous environments, [22] with products generated that are hydrolytically robust. This tyrosine labelling strategy has been employed in protein bioconjugation, [23] DNA modification, [24,25] and the synthesis of glycoconjugate vaccines. [26]

In the design of drug delivery systems, the end-functional block copolymers, especially telechelic polymers are particularly interesting as they offer a feasible approach to introduce two different biologically active entities at the two chain-ends, such as drugs, targeting ligands, imaging agent or other biological relevant properties. [27] The synthesis approaches for functionalized telechelic polymers have been extensively studied, such as a heterotelechelic polyacrylamide (PAAm) bearing biotin and doxorubicin (Dox) at each chain-end was synthesized by reversible addition–fragmentation chain transfer (RAFT) polymerization. [28] Here,

the phenol-PTAD reaction is demonstrated as an outstanding method for facile and rapid polymer conjugation to produce a heterotelechelic block copolymer under aqueous conditions. This method was used for the preparation of block polymers that generated stimuli sensitive multifunctional nanoparticles and allowed the inclusion of targeting ligands and optical tags to allow analysis of their biodistribution and target accumulation as well as on-demand release. The delivery system showed exquisite and physiologically relevant pH-directed morphological alteration of the structure of the nanoparticle.

EXPERIMENTAL SECTION

General Information All reagents were obtained from Sigma Aldrich and used as received. Polyethylene glycol methacrylate was purchased from Sigma Aldrich and was found to have a PDI of 1.08 (GPC) with molecular weight range from M_n = 255Da - 682Da, n= 4 - 14 from MALDI) (see supporting information). LysoTrackerTM and CellTrackerTM Green were obtained from ThermoFisher. Reactions, which required oxygen and moisture free conditions, were carried out with using Schlenk techniques under a nitrogen atmosphere. ^{1}H and ^{13}C nuclear magnetic resonance spectra were recorded on a Bruker AVA500 spectrometer (500 and 125 MHz respectively) at 298 K in deuterated solvents. Coupling constants were measured in Hertz (Hz). Chromatographic purifications were carried out on silica gel 60-120 mesh. Analytical thin layer chromatography was performed on silica gel F254 (Merck). Low Resolution Mass Spectra were obtained using a Hewlett Packard LCMS 110 ChemStation with a G1946B mass detector. Polymers were analysed by gel permeation chromatography (GPC) using two PLgel MIXED-C columns (200 - 2,000,000 g mol-1, 5 µm) using N, N-dimethylformamide (DMF) with 0.1M LiBr at 60 ^{o}C at 1 mL min^{-1} as the eluent. The GPC was calibrated with PMMA and PEG as

standards. DLS (dynamic light scattering) measurements were carried out on a Malvern Zetasizer

NanoZS at 25 ºC. Transmission Electron Microscope (TEM) analyses were conducted with

JEOL JEM-1400 Plus at Welcome Trust of Biology Image Centre of Edinburgh.

Synthesis of Sulfo-Cy5-alkyne 7

Sulfo-Cy5-carboxylic acid

7
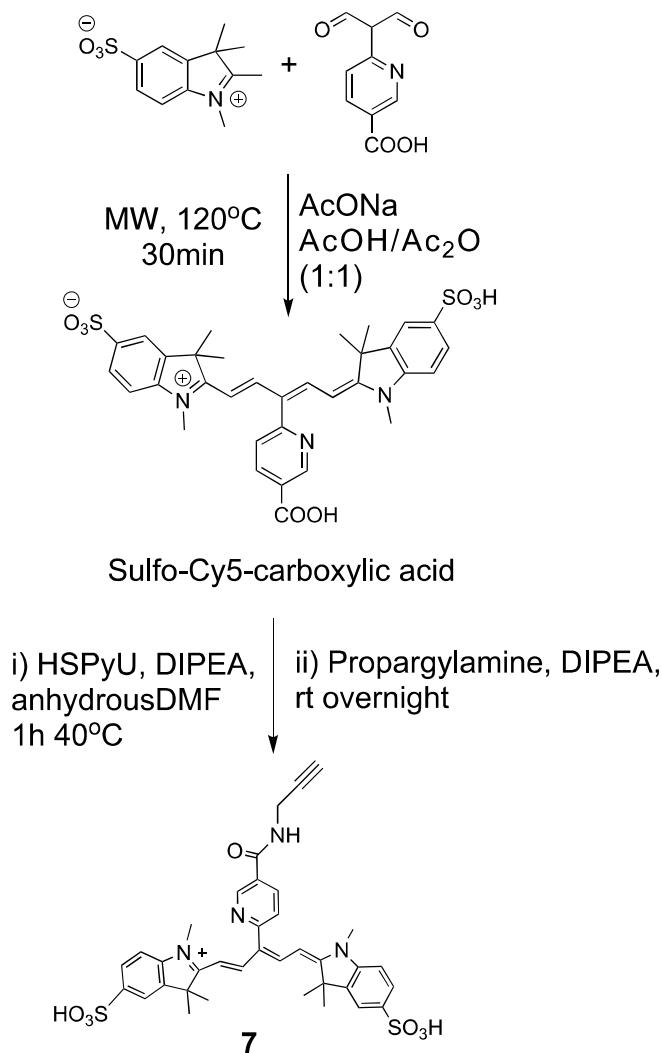
Synthesis of sulfo-Cy5-carboxilic acid A solution of 1,2,3,3-tetramethyl-3H-indolium 5-

sulfonate[29] (372 mg, 1.47 mmol, 2.2 eq), 6-(1-formyl-2-oxoethyl)-3-pyridinecarboxylic acid (129

mg, 0.67 mmol, 1.0 eq) and sodium acetate (346 mg, 4.22 mmol, 6.3 eq) in acetic

anhydride/acetic acid (1:1, 10 mL) was added to a microwave vial and heated at 120°C for 30

minutes. The mixture was cooled to room temperature and the solvents were removed under *in*

vacuo. Cold diethyl ether was added and the precipitated solid collected by centrifugation and washed with diethyl ether (3x15mL). The obtained solid was dried under vacuum (351mg, 75%); ^{1}H NMR (500 MHz, DMSO-d$_6$) δ: 9.19 (s, 1H), 8.44 (d, J = 14.3 Hz, 2H), 8.31 (d, J = 7.8 Hz, 1H), 7.83 (s, 2H), 7.64 (d, J = 8.2 Hz, 2H), 7.42 (d, J = 7.8 Hz, 1H), 7.30 (d, J = 8.3 Hz, 2H), 5.83 (d, J = 14.3 Hz, 2H), 3.35 (s, 6H), 1.77 (s, 12H); ^{13}C NMR (125 MHz, CD$_3$OD) δ: 172.1, 157.1, 154.7, 152.2, 145.4, 143.8, 142.6, 139.8, 134.1, 128.0, 126.8, 121.2, 111.7, 102.7, 50.8, 31.7, 27.5; HR-MS (ESI): cal. C$_{33}$H$_{32}$O$_8$N$_3$S$_2^-$ 662.1636; found: 662.1651 (M)$^-$

Sulfo-Cy5-Carboxylic acid (75 mg, 0.11 mmol) was dissolved in anhydrous DMF (8 mL). HSPyU (46 mg, 0.11 mmol) and DIPEA (58 µL, 0.33 mmol) were added and the mixture stirred at 40°C for 1h. Propargylamine (30 mg, 0.55 mmol) was added together with DIPEA (58 µL, 0.33 mmol) and the reaction was stirred overnight. The solvent was removed under vacuum. Purification by column chromatography (10:1 ACN-H$_2$O) afforded the compound Sulfo-Cy5-alkyne as a dark blue solid (55 mg, 70%). ^{1}H-NMR (500 MHz, DMSO-d$_6$) δ: 9.28 (t, J = 5.5 Hz, NH), 9.23 (d, J = 2.3 Hz, 1H), 8.47 (s, 1H), 8.44 (s, 1H), 8.38 (dd, J = 8.1, 2.3 Hz, 1H), 7.84 (s, 2H), 7.64 (m, 3H), 7.32 (d, J = 8.3 Hz, 2H), 5.84 (m, 2H), 4.15 (dd, J = 5.5, 2.5 Hz, 2H), 3.38 (s, 6H), 3.20 (t, J = 2.5 Hz, 1H), 1.78 (s, 12H); ^{13}C-NMR (125 MHz, , DMSO-d$_6$) δ: 174.2, 164.2, 157.3, 152.2, 149.0, 145.6, 142.4, 140.4, 135.9, 127.6, 125.8, 125.2, 119.7, 110.2, 100.7, 80.9, 73.0, 49.0, 31.0, 28.4, 26.7; HPLC t$_R$ 3.921 min (650 nm); HR-MS (ESI): cal. C$_{36}$H$_{37}$O$_7$N$_4$S$_2^+$ 701.2098; found: 701.2068 (M)$^+$.

Synthesis of alkyne functionalized folic acid (FA-alkyne) 8[30,31] 10 mL DMF containing 0.5 g folic acid was cooled in a water/ice bath. *N*-hydroxysuccinimide (130 mg) and EDC (220 mg) were added and the resulting mixture was stirred in the ice bath for 30 min. Then 2.5 mL DMF containing propargylamine (62 mg) was added and the reaction system was stirred for another 24

h at room temperature. The precipitation was filtered, washed with acetone and dried under vacuum oven overnight. ^{1}H NMR (500 MHz, DMSO-d_6): 8.61 (s, 1H), 8.28–8.23 (d, 1H, J = 5.3 Hz), 8.06–8.04 (d, 1H, J = 7.5 Hz), 7.66–7.63 (d, 2H, J = 8.3 Hz) 6.93 (br s, 2H), 6.65–6.62 (d, 2H, J = 8.2 Hz), 4.53–4.51(d, 2H, J = 5.2 Hz), 4.30–4.28 (m, 1H), 3.83–3.80 (m, 2H), 3.05–3.03 (t, 1H, J = 2.5 Hz), 2.82 (s, 1H), 2.68 (s, 1H), 2.31 (m, 2H), 1.92–1.90 (m, 1H), 1.85–1.82 (m, 1H).

General procedure of polymerization Poly (ethylene glycol) methylacrylate (1.5 mL, 3.2 mmol), initiator 1 (7.9 mg, 0.032 mmol), 2,2'-bipyridine ligand (14.3 mg, 0.064 mmol) were charged into a dry Schlenk tube along with toluene (1 mL) and subjected to three freeze-pump-thaw cycles. This solution was cannulated under nitrogen into a second Schlenk tube, previously evacuated and filled with nitrogen, containing Cu(I)Br (4.4 mg, 0.032 mmol) and a magnetic follower. The reaction was heated to 55 ^{o}C with constant stirring. After 18 h, the mixture was diluted with 20 mL of toluene and air was bubbled through for 4 h. The reaction mixture was passed through a short neutral alumina column and subsequently washed with toluene. The volatiles were removed under reduced pressure and the residue dissolved in THF (ca. 5 mL) prior to precipitation by diethyl ether (ca. 100 mL). The white solid was isolated by filtration, washed with additional diethyl ether and volatiles were removed under reduced pressure to give polymer **1**.

Synthesis of polymer 4 TMS-alkyne-PEG (3) (150.0 mg, 2 mM, prepared by ATRP polymerisation as described above see supporting information for the details), and TBAF (3 mM, 200 mM in THF) were dissolved in THF (1.97 mL). The reaction mixture was allowed to stir overnight at room temperature. The formed polymer was precipitated by addition of cold Et$_2$O and the white solid was isolated by filtration, washed with additional Et$_2$O. The obtained product

was placed under reduced pressure for overnight. PEG-alkyne (180.0 mg, 2.4 mM), PTAD-azide (3.2 mg, 6 mM), sodium ascorbate (3.8 mg, 9.6 mM) and $CuSO_4$ (1.1 mg, 6.8 mM) were placed into a 5 mL flask along with 2 mL methanol. The reaction mixture was stirred for overnight at room temperature and dialysed against distilled water for 48 h followed by freeze-dry to obtain PEG-PTAD (135.0 mg, yield 90%).

PEG-PTAD (60 mg, 0.26 mM solution in DCM) was added to 1,3-dibromo-5,5-dimethylimidazolidine-2,4-dione (6 mg, 2.6 mM). The reaction mixture was stirred and formation of a light pink colour was observed, characteristic for the presence of the desired PTAD reagent. After 2 h, silica sulfuric acid (SiO_2-OSO_3H) 4 times weight to starting materials) was added and stirred at room temperature for half an hour. The silica sulfuric acid was removed by centrifugation and the volatile materials removed *in vacuo* to give polymer **4** (quantitative yield).

General procedures of polymer-polymer coupling through PTAD-phenol reaction All the polymer-polymer coupling reactions followed the same conditions except for the specific pH required for each reaction. Taking polymer **4** coupling **6** as an example: A solution of **4** (1.00 mL, 0.52 mM) in pH 4.0 Citric acid buffer was added into a solution of **6** (1.00 mL, 0.52 mM) pH 4.0 citric acid buffer) and the mixture was stirred at room temperature in the dark. After half an hour, the reaction mixture was dialysed against water for 48 h followed by freeze-dring to give **4-*b*-6** (quantitative yield).

Synthesis of Cy5-4-b-6 A solution of sodium azide in methanol (3.48 mM, 2 mL) was added to a solution of 4-*b*-6 in methanol (0.87 mM, 2 mL). The mixture was stirred overnight in dark. The solution was dialysed against water for 48 h followed by freeze drying to give azide-4-b-6. Azide-4-*b*-6 (0.65 mM), Cy5-alkyne 7 (2.3 mg, 1.64 mM), sodium ascorbate (1.0 mg, 2.6 mM)

and $CuSO_4$ (0.3 mg, 0.98 mM) were mixed in methanol (2 mL). The reaction mixture was stirred overnight at room temperature in dark and then dialysed against distilled water for 48 h followed by freeze drying to give **Cy5-4-b-6** (9.2 mg, yield 85%).

Synthesis of Cy5-4-b-6-azide A solution of sodium azide in methanol (3.48 mM, 2 mL) was added to a solution of Cy5-4-b-6 in methanol (0.87 mM, 5 mL). The mixture was stirred overnight in dark, the solution was dialyzed against water for 48 h followed by freeze dry to give azide functionalized **Cy5-4-b-6-azide** (quantitative yield).

Synthesis of Cy5-4-*b*-6-FA Azide functionalized Cy5-4-*b*-6-azide (150.0 mg, 1.5 mmol), FA-alkyne (3.9 mg, 4.4 mmol), sodium ascorbate (2.3 mg, 6.0 mmol) and $CuSO_4$ (1.0 mg, 4.0 mmol) were stirred in methanol (2 mL). The reaction mixture was stirred overnight at room temperature in the dark before dialysis against distilled water for 48 h followed by freeze-dry to give **Cy5-4-*b*-6-FA** (122 mg, yield 81%).

Characterization of the cargo loaded nanoparticles To determine the DOX content, a calibration of DOX fluorescence against DOX concentrations ranging from 0.05 to 10 µg/mL was determined (excitation wavelength: 505 nm; emission wavelength: 565 nm). Subsequently, 9 mL of DMSO was added to 1 mL of the DOX loaded nanoparticle to extract the DOX encapsulated from the nanoparticles. The DOX concentration (C) was determined following a 10-fold dilution of the extraction. The encapsulation efficiency (EE %) of the DOX loaded nanoparticle was calculated using the formula $(C \times V)/m$, where C represents the DOX concentration in the DOX loaded nanoparticle solution, m represents the amount of DOX used (which was 2 mg in this experiment), and V represents the total volume of the DOX loaded nanoparticle solution in mL. The determination of the Nile Red content followed the same

procedure except for the set of the fluorescent photometer (excitation wavelength: 530 nm; emission wavelength: 590 nm).

The study of release profiles The fluorescent intensity of Nile Red-loaded nanoparticles (Nile Red concentration: 10 µg/mL) solution and the Nile Red in pH 7.4 PBS buffer at a concentration of 10 µg/mL were measured using a plate reader (excitation wavelength: 530 nm; emission wavelength: 590 nm), cited as A_0 and A_1, respectively. Glucono-δ-lactone (GdL) powder (100 mM) was added to the Nile Red-loaded nanoparticles (Nile Red concentration: 10 µg/mL) solution and at pre-determined time points, the fluorescent intensity of the Nile Red-loaded nanoparticles solution with or without Gdl were measured. (A) The cumulative release percentage of the Nile Red-loaded nanoparticles was calculated from the formula $(A-A_0)/ (A_1-A_0) \times 100$ %. All the experiments were performed three times. The pH of the nanoparticle solution with Gdl was determined using a pH meter at 10 min intervals.

Cell culture HeLa and KB cells in DMEM were maintained at 37 °C in a humidified atmosphere containing 5 % CO_2. All media were supplemented with 10 % (v/v) FBS and penicillin/streptomycin (100 $U \cdot mL^{-1}$ of each). The cells were regularly sub-cultured using trypsin/EDTA.

Cellular uptake of the cargos loaded nanoparticles HeLa or KB cells were seeded in 24-well plate at a density of 5×10^4 cells/well. After attachment, the cells were treated with test agents (at a final polymer concentration of 20 µg/mL) for different time periods. The nuclei were labelled with Hoechst 33342. After washing the cells three times with PBS, the cells were observed by fluorescent microscopy. For the folic acid (FA) blocking experiment, free FA (90 µg/mL) was added to the medium 30 minutes before the exposure to the test agents.

Cytotoxicity of the blank and DOX loaded nanoparticles HeLa or KB cells were seeded in 96-well Lab-Tek II chambers at a density of 5×10^4 cells per chamber and allowed to attach overnight. The cells were exposed to a series of concentrations of the blank and DOX-loaded micelles for 48 h. Subsequently, the cells were incubated with 20 μL of a 3-(4,5-dimethylthiazol-2-yl)-2,5-diphenyltetrazolium bromide (MTT) solution (5 mg/mL) per well for an additional 4 h at 37 °C. At the end of the incubation period, 100 μL DMSO was added to each well to replace the culture medium and dissolve the insoluble formazan crystals. The plate was shaken for 30 min, and the optical density was determined at 570 nm using a plate reader (Bio-Rad, Model 680, USA). Cell viability was calculated in reference to cells incubated with culture medium alone. All of the experiments were repeated six times.

Intracellular release behaviour of the Nile Red-loaded nanoparticles HeLa Cells were seeded in 24-well Lab-Tek II chamber slides at a density of 5×10^4 cells/well. After attachment, the cells were treated with Nile Red-loaded nanoparticles (Cy5-4-*b*-6-FA) (at a final polymer concentration of 20 μg/mL) for different time periods (8 h, 12 h, and 48 h). The nuclei were labelled with Hoechst 33342 and the acidic lysosomes were stained with Lysotracker according to the manufacturer's protocol. After washing the cells three times with PBS, the cells were fixed in 4% paraformaldehyde solution at room temperature for 30 min and then observed using a confocal laser-scanning microscope.

Release in HeLa spheroids. HeLa cells were maintained at 37ºC / 5% CO2 in DMEM containing 1% penicillin-streptomycin and supplemented with 10% FBS and 1% glutamine. To produce 3D cellular aggregates, cellular suspensions were formed using trypsin-EDTA. Approximately 2000 HeLa cells were then seeded into 96 well u-bottomed Nunclon™ Sphera™ Microplates (Thermofisher) in 100μl of media. The mircoplate plate was spun for 5 minutes at

200 x G and maintained at 37ºC / 5% CO2 for four days. After four days of incubation Nile Red labelled nanoparticles (**Cy5-4-*b*-6-FA**) were added to each well to a concentration of 20µg (1 in 100 dilution of stock) and the cellular aggregates cultured for a further 2 days. The media containing the Nile Red labelled nanoparticles was then removed and aggregates incubated with 70 nM of Lysotracker Green 40 minutes at 37 ºC and with Hoechst 33342 for 10 mins at 37 ºC. Cells aggregates were then fixed in 4% PFA for 20 minutes at room temperature and washed three times in PBS before being mounted onto glass slides in ProLong™ Gold Antifade Mountant (Thermofisher) and covered with coverslips. Multiple replicates were performed in three repeated experiments.

RESULTS AND DISCUSSION

Polymer conjugation involving the reaction of a PTAD conjugated polymer and a phenol derivatized polymer as illustrated in Scheme 1. As a proof-of-concept, the orthogonality of this reaction with respect to commonly utilized initiators and catalysts in atom transfer radical polymerization (ATRP) and in PBS (pH 7.4) was studied.[32] Thus 4-hydroxyphenyl 2-bromoisobutyrate (initiator A) was synthesized as an ATRP initiator. The polymer bearing a terminal phenol (**1**) was prepared by polymerization of poly (ethylene glycol) methacrylate (PEGMA) through ATRP with M_n = 10.7 KDa and PDI = 1.25. Polymer (**2**) was obtained from the deprotection of polymer (**3**) which was prepared via ATRP polymerization of PEGMA using initiator B. PTAD-Polymer (**4**) was synthesized by a Cu catalyzed alkyne-azide cycloadditon (CuAAC) reaction between alkyne terminated polymer (**2**) and (**5**) followed by oxidation (see Scheme 1).

Polymer (**1**) was observed to rapidly react with PTAD-Polymer (**4**) at room temperature in PBS at pH 4.0, 7.4 and 9.2 (see Scheme 1) as evidenced by size exclusion chromatography (SEC) and with SEC traces showing a quantitative generation of polymer (**1-*b*-4**) (see Figure 1).

Among the different types of stimuli, pH sensitive systems have been amongst the most widely used to design nanoparticles applied in drug delivery.[33] Thus our conjugation strategy was used to link a pH sensitive block copolymer (poly(diethylaminoethyl methacrylate) (pDEAEMA) to the PEGMA based hydrophilic block. Phenol terminated pDEAEMA (**6**) was prepared by ATRP using initiator A. pDEAEMA (**6**) reacted with PTAD functionalized polymer (**4**) with quantitative conversion within 30 mins at pH 4.0 at room temperature, giving the block copolymer (**4-*b*-6**), with a M_n of 11.9 kDa and a PDI of 1.23 (see Table 1 and Figure S7). NMR diffusion experiments (DOSY) were performed on an equimolar mixture of polymer (**4**) and (**6**) to provide further evidence for the polymer conjugation. The resulting block copolymer (**4-*b*-6**) move through solution as one molecular specie with a diffusion coefficient (log D = 10.537 $m^2 S^{-1}$), which was different from that of the polymers (**4**) and (**6**) (log D = 10.613 $m^2 S^{-1}$ and 10.359 $m^2 S^{-1}$, respectively) (Figure S12).

The left over bromo group from the ATRP initiator could be converted into an azido group by reacting with sodium azide, to give polymers that would offer further opportunities for the attachment of both fluorescent tags and cellular targeting ligands via azide/alkyne conjugation chemistry (see Scheme 1).

To generate well-defined multi-functionalised block copolymers, the bromo group (remaining from the initiator) of pDEAEMA (**6**) was converted to an azido group prior to conjugation with polymer 4, thus afforded polymer (**4-*b*-6-azide**, Scheme 2). Here folic acid (FA) was utilized as a targeting ligand as folate receptors are overexpressed on many tumour types,[34-36] while sulfo-

Cy5-carboxylic acid was used as a fluorescent reporter. Thus Cy5-alkyne (7) was treated with the azide terminated polymer (**4-*b*-6-azide**) through a CuAAC reaction to afford (**Cy5-4-*b*-6**) (see Scheme 1). The bromide in Cy5-4-*b*-6 was itself then displaced with an azide to give (**Cy5-4-*b*-6-azide**) followed by another CuAAC reaction with an alkyne functionalized folic acid (**6**) to give (**Cy5-4-*b*-6-FA**).

The block copolymer (**Cy5-4-*b*-6-FA**) dissolved in pH 4.0 phosphate-citrate buffer since the PEG block is hydrophilic and the amines protonate. When the pH was adjusted (> 7.4) nanoparticles with a diameter of 140 ± 32 nm and PDI = 0.112 were formed (as analyzed by dynamic light scattering (DLS)), with transmission electron microscopy (TEM) showing a characteristic solid core morphology with average diameter 121 nm (Figure 2). The formation of this compartmentalized self-assembled structure was postulated to be due to the presence of non-protonated tertiary amine residues along the pDEAEMA block (pKa 6.5-6.9 depending on the molecular weight[37,38]), which forms an amphiphilic block copolymer with the hydrophilic PEG block. An MTT assay was used for quantitative testing of the viability of HeLa cells in the presence of NPs, with low inhibitory concentrations (IC_{50}) of NPs against HeLa and HEK cells was determined to be ~22 mM, suggesting a fairly low cytotoxicity (see Figure S17). When the pH was adjusted back to 4.0, the particles disassembled as evidenced by TEM (no nanostructures were observed) and DLS where the polymer remained in a unimer state. Polymer (**4-*b*-6**), also exhibited large changes in absorbance at different pH, with absorbance increasing sharply when the pH changed from 6.0 to pH 7.4, indicating nanoparticle self-assembly (Figure S14).

The release of encapsulated Nile Red from the nanoparticles at different pH was investigated with the pH controlled in a smooth and reproducible manner, via the slow hydrolysis of glucono-δ-lactone to gluconic acid.[39,40] A solution of glucono-δ-lactone (10 mM) exhibited an initial pH

of 7.0 which dropped to pH 3.0 over 2 hours where it remained constant. Figure 3 shows the release profile of the dye in the presence of glucono-δ-lactone, with quantitative release within 4 hours, attributed to protonation of the pDEAEMA block and disassembly of the nanoparticles (Figure 3a). Three dimensional cell culture models have been developed to bridge the gap between 2D cell-based assays and *in vivo* studies. In this study, HeLa spheroids were used to investigate cargo liberation in a 3D environment, with the nanoparticles penetrating into the spheriods and efficiently releasing Nile Red (Figure 3b).

To explore the NPs as a drug carrier, doxorubicin (DOX) was also encapsulated. The release profiles were evaluated at different pH (see Figure 3c) with 40% release observed at pH 7.4 and 80% at pH 4.0, after 20 hours at 37 ºC. The drug release at pH 7.4 could be potentially controlled through further modification to the nanoparticles to enhance drug retention and enable tailorable release kinetics, such as shell cross-linked (SCL) or core cross-linking strategies, or via covalent attach (pro-) drug molecules in the micellar core,[41-43] however, which was not pursuit in the current study.

DOX loaded (**Cy5-4-*b*-6-FA)** and (**Cy5-4-*b*-6)** nanoparticles were prepared. To visualise the effect of folate-mediated uptake of the nanoparticles, FR-positive cell lines (KB and HeLa) were studied. Nanoparticle uptake was found to be time-dependent with the (**Cy5-4-*b*-6-FA)** nanoparticles exhibiting faster cellular internalization behavior than the equivalent (non-folate) (**Cy5-4-*b*-6)** nanoparticles, while cells pretreated with folic acid showed reduced cellular uptake, indicating folate-mediated uptake (Figure 4). The IC50 values of DOX loaded (**Cy5-4-*b*-6-FA)** nanoparticles against HeLa and KB cells were 1.8 $\pm$ 0.1 μg/mL and 1.2 $\pm$ 0.09 μg/mL, respectively when compared to IC50 values of 3.8 $\pm$ 0.2 μg/mL against HeLa cells and 2.2 $\pm$ 0.14 μg/ml against KB cells using the NPs (**Cy5-4-*b*-6)** without folate conjugation.

It is known that the pH in the endosome is in the range from 5.5 to 6.8,[44] while in the lysosome it is between 4.0 and 5.0,[45] and this intrinsic pH gradient has been used to design nanoreporters for the imaging of cellular compartments.[46] pDEAEMA containing nanoparticles have been used as drug carriers and their fusogenic activity reported, with destabilization and/or fusion with the endosomal membrane allowing efficient cargo release into the cytoplasm.[47]

To evaluate the fate of the NPs and cargo release in cells, NPs were loaded with Nile Red and incubated with HeLa cells. Figure 5b shows that after 12 h Nile Red was predominantly co-localized in LysoTraker co-labelled acidic organelles (green). After 48 h the Nile Red was found, not only in the acidic regions but also throughout the rest of cell. However, the NPs were only detected in the lysosomes after 48 h (Figure S22), suggesting that the NPs were located lysosomes after cellular internalization. After active internalization, the nanoparticle targeting actions of folic acid combined with the pH-triggered drug release mediated by the endosomal pH results in the disassembly of nanoparticles.

CONCLUSIONS

In summary, the utility of the highly efficient phenol-PTAD conjugation reaction as applied to polymer end-modification and polymer-polymer conjugation in aqueous solutions. The targeted and fluorescently labeled multifunctional pH responsive block copolymer PEG-*b*-PDEAMA was successfully prepared based on this strategy. The amphiphilic block copolymer easily under went self-assembly *in situ* when the pH was adjusted to physiological pH (~7.4) and above to achieve nanoparticles with the desired surface ligand (folic acid) and fluorescent probe (sulfo-Cy5). It was successfully demonstrated that the folic acid modified multifunctional nanoparticles

promoted cellular uptake, with the fluorescence tagged NPs localized in the endo-lysosomes

determined. The polymeric nanoparticles successfully encapsulated Nile Red and DOX which

were rapidly released in response to an acidic stimuli intracellularly. Previous studies revolved

that the fusogenic activity of protonated tertiary amines can interact and stimulate fusion or

destabilization of target membranes promoting efficient endosome drug escape.[48] Thus, one of

our future research will be to investigate the role of pDEAEMA in the disruption of lysosomal

structure and NPs lysosomal escape. In addition, the nanoparticles remain stable for > 2 months

in PBS (pH 7.4) under ambient conditions. Beyond the pH sensitive polymers demonstrated here,

this polymer conjugation strategy could easily be adjusted to allow the generation of

multifunctional polymers using other type of responsive monomers. Our method provides a

powerful strategy to conjugate multiple polymer components, while allowing their tagging with

both ligands and fluorescent reporters and thus allows, as demonstrated here, the generation and

functionalization of a variety of polymer-based nanosystems for diverse biomedical applications.
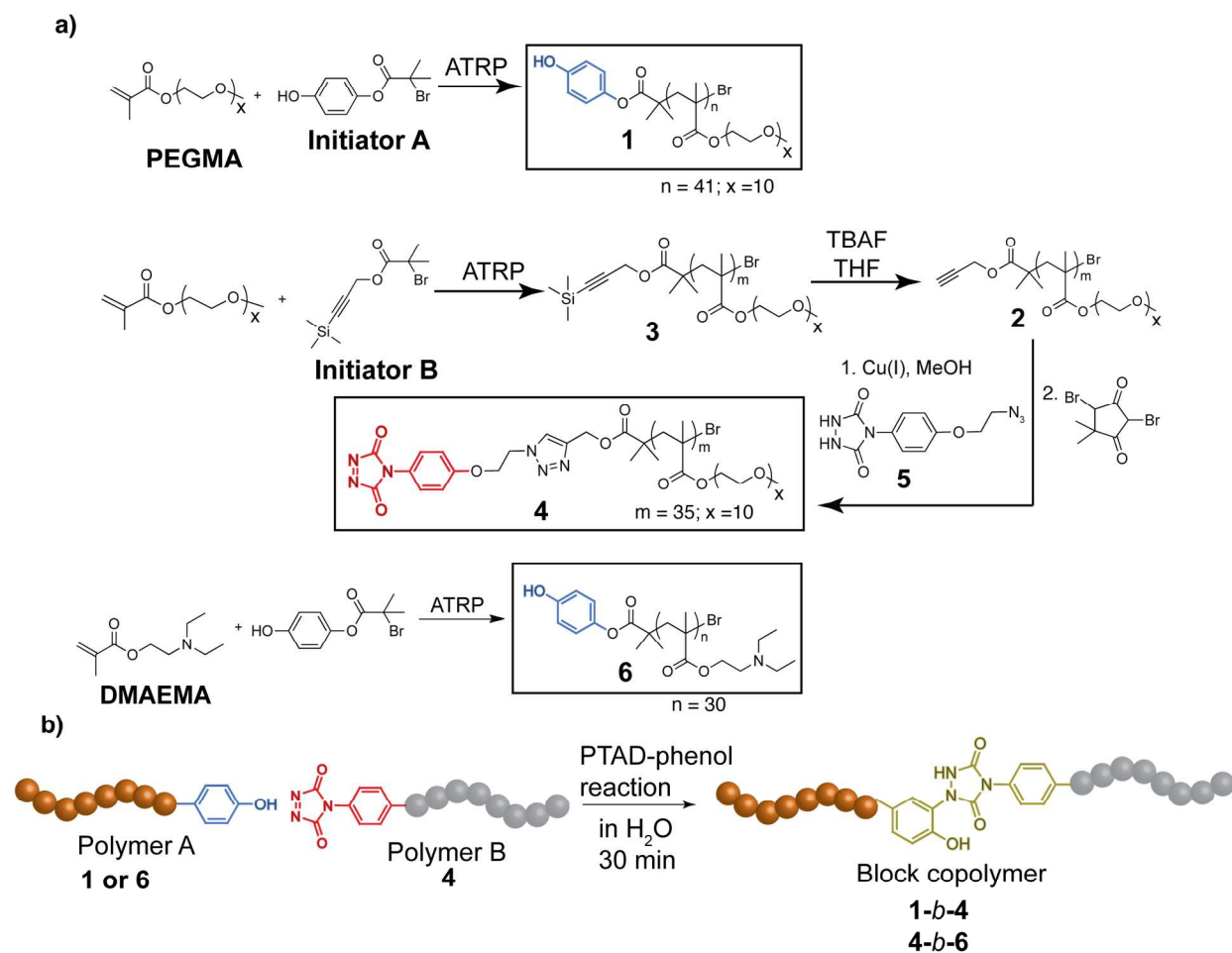
Scheme 1. a) Synthesis of phenol terminated polymers (**1** and **6**) and PTAD-Polymer (**4**); b).

Polymer-Polymer coupling through PTAD-phenol conjugation chemistry.
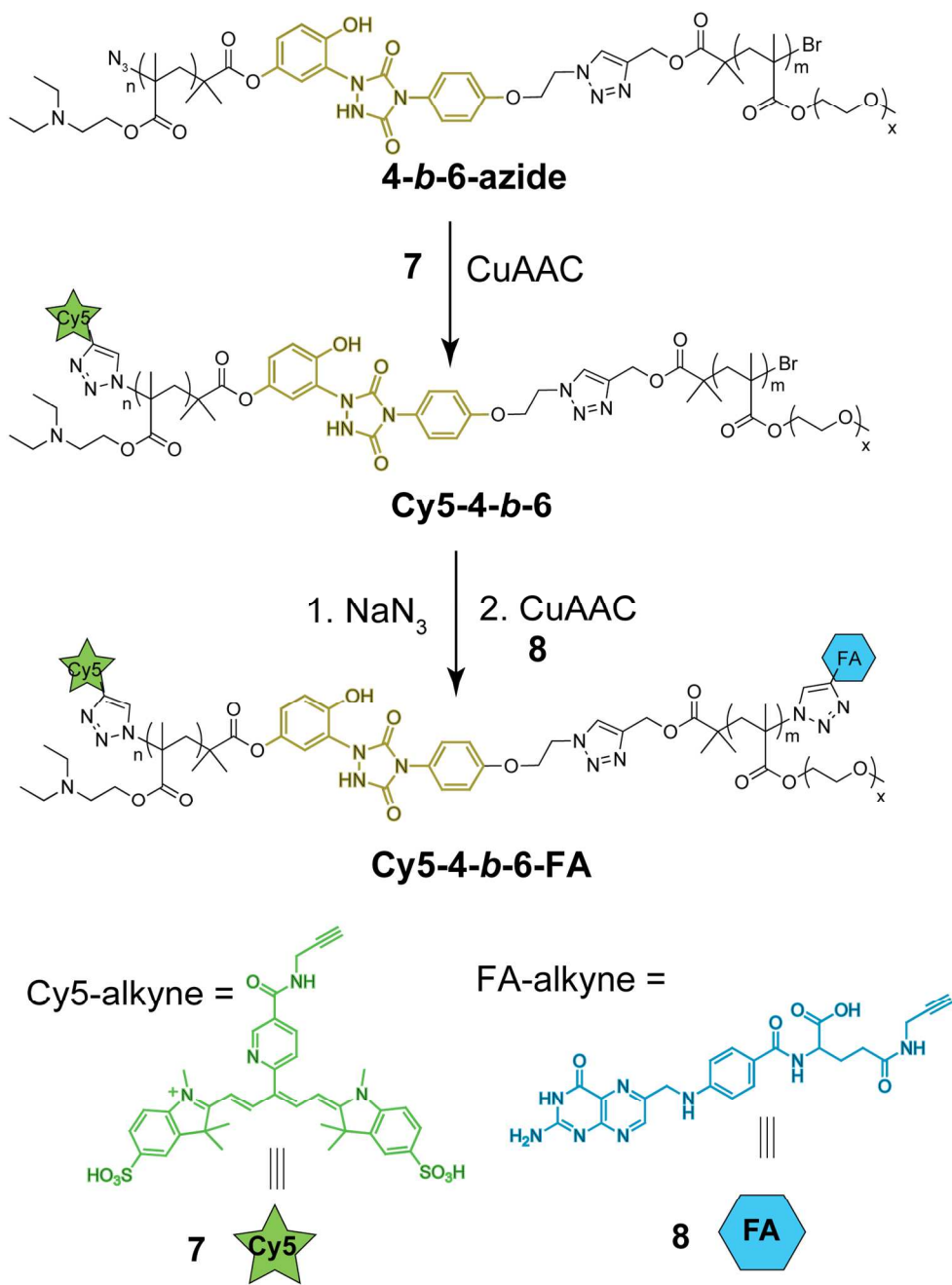
Scheme 2. Synthesis of block copolymer (**Cy5-4-*b*-6-FA**) with Cy5 and folic acid functionalization through the combination of CuAAC and PTAD-phenol conjugation chemistries.
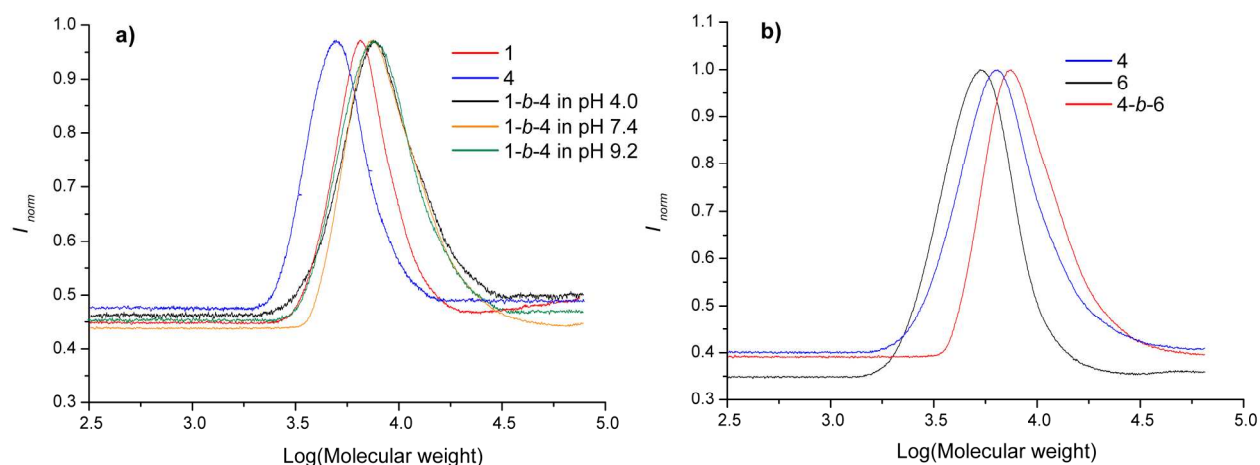
Figure 1. SEC traces of reaction between polymer (**1**) or (**6**) and (**4**): a) polymer (**1**-***b***-**4**) by the reaction of (**1**) and (**4**) at pHs 4.0, 7.4 and 9.2; b) polymer (**4**-***b***-**6**) by the reaction of (4) and (6) at pH 4. All reactions were carried out in 10 mM aqueous b buffer solution (pH 4.0 phosphate-citrate buffer, pH 7.4 PBS, and pH 9.2 carbonate-bicarbonate buffer) for 30 mins at room temperature. SEC eluting with DMF with 1% LiBr at 60 ºC with a refractive index detector (calibrated with PEG and PMMA standards).
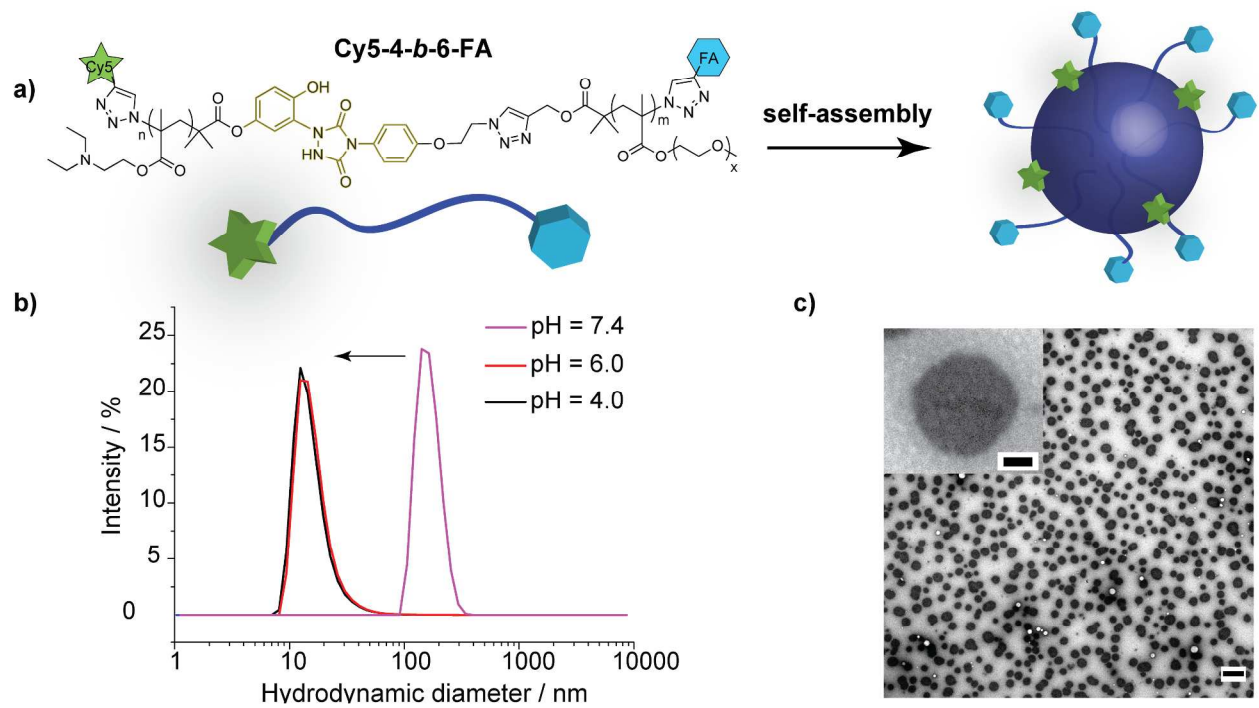
Figure 2. a). Sulfo-Cy5 (**7**) and folic acid (**8**) functionalized block co-polymer (**Cy5-4-b-6-FA**)

self-assembly into nanoparticles with folic acid (stars) and sulfo-Cy5 (hexagon). b).

Hydrodynamic diameter of nanoparticles at pH 7.4, 6.0 and 4.0. c) TEM image of nanop

nanoparticles (**Cy5-4-b-6-FA**) prepared at pH 7.4, inset shows a single nanoparticle (scale bar =
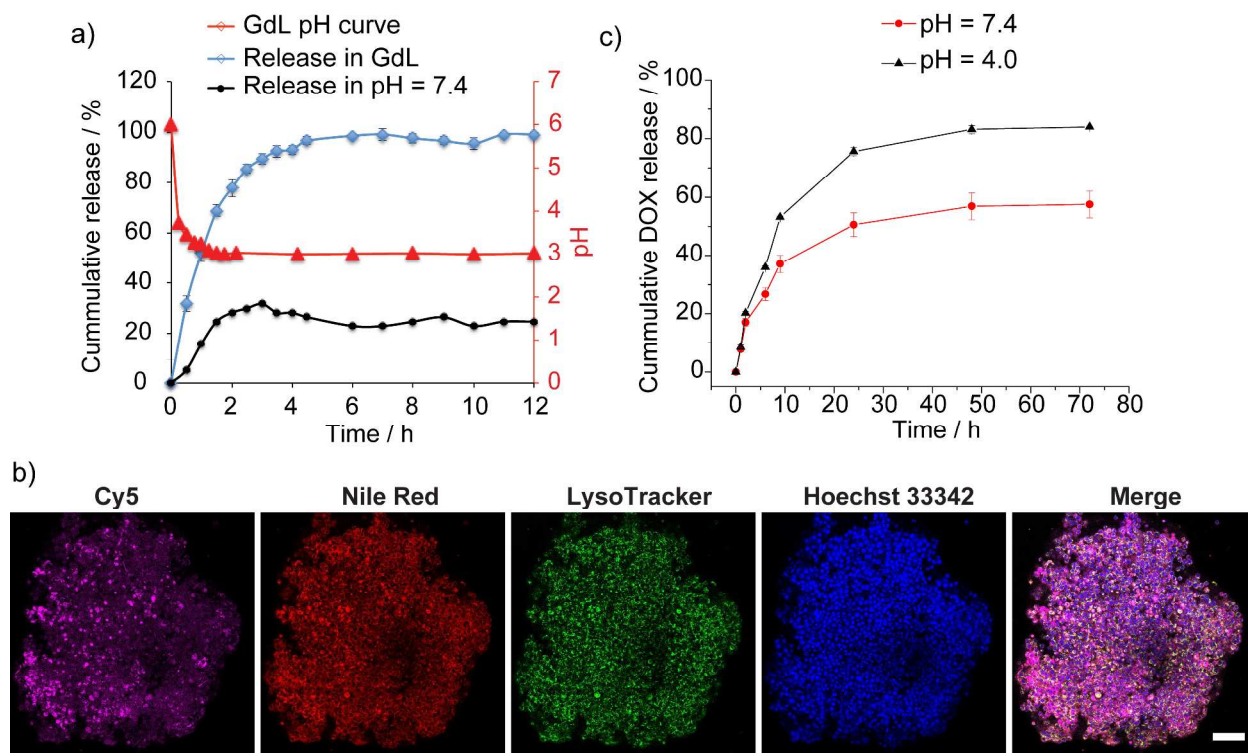
200 nm; inset = 20 nm).

Figure 3. a). Evolution of pH over time (red axis), and release of Nile Red from the nanoparticles (left Y-axis) in the presence and absence of glucono-δ-lactone (GdL) (10 mM) (right axis and the red line is the pH change); b) Confocal microscope images of distrib distribution of Nile red loaded NPs in HeLa spheroids. NPs (purple, λ_{ex} = 650 nm; λ_{em} = 670 nm), Nile Red (red, λ_{ex} = 530 nm; λ_{em} = 635 nm), Hoechst 33342 (blue, λ_{ex} = 358 nm; λ_{em} = 461 nm) for nuclei staining and LysoTracker (green, λ_{ex} = 530 nm; λ_{em} = 590 nm). Scale bar = 100 μm. c.) Drug release profiles of the DOX loaded NPs in pH 7.4 and 4.0.

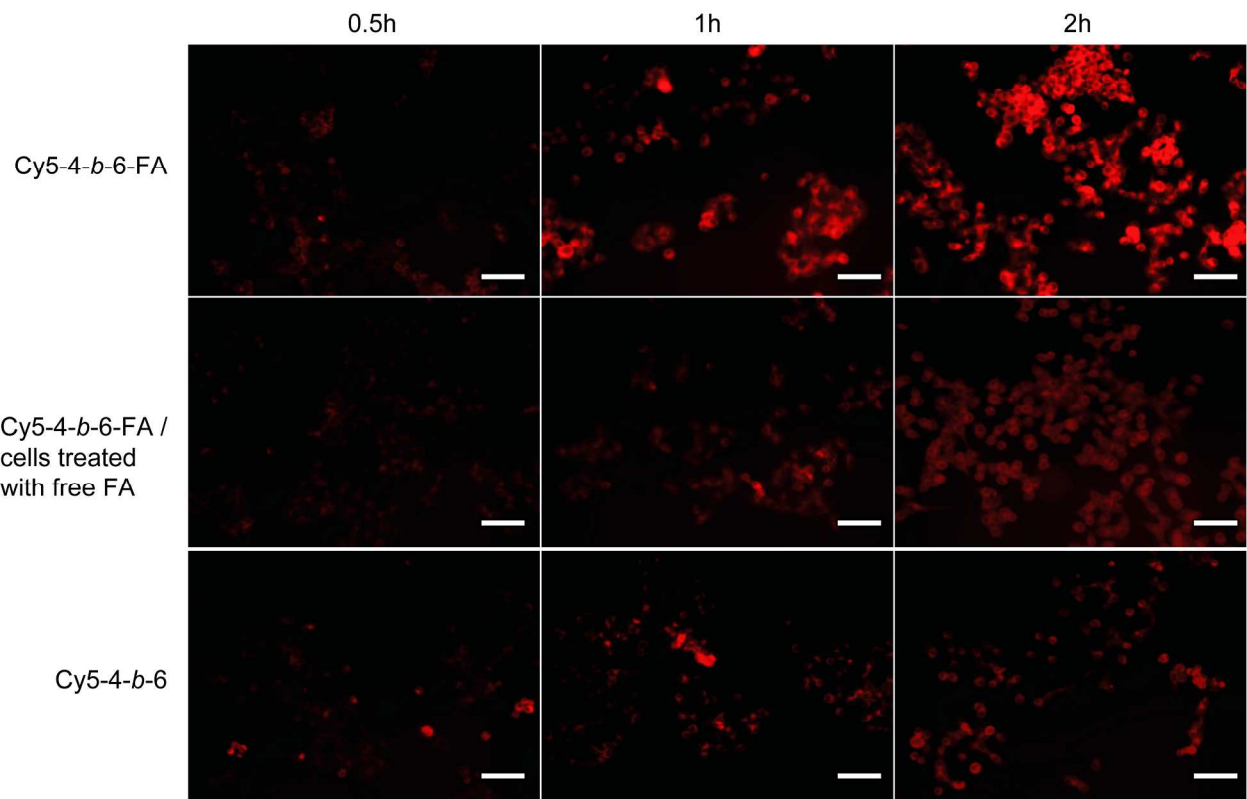**Figure 4.** The fluorescent images of KB cells after incubated with the NPs for 0.5 h, 1h and 2 h

(λ_{ex} = 550 nm; (λ_{ex} = 570 nm). Top: cells incubated with nanoparticles functionalized with folic

acid (**Cy5-4-*b*-6-FA**); middle: cells were treated with free folic acid (90 μg/mL) prior to

incubation with folic acid functionalized nanoparticles (**Cy5-4-*b*-6-FA**); bottom: cells incubated

with nanoparticles without folic acid functionalization (**Cy5-4-*b*-6**). Scale bars = 100 μm.

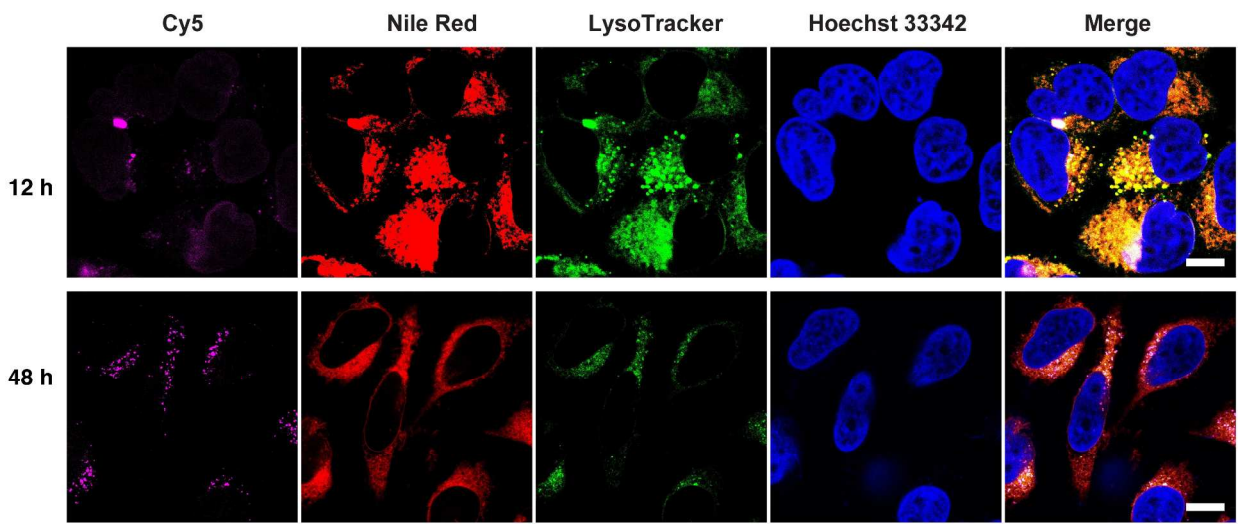**Figure 5.** Confocal microscope images of distribution of NPs (purple, λ_{ex} = 650 nm; λ_{em} = 670 nm) loaded with Nile Red (red, λ_{ex} = 530 nm; λ_{em} = 635 nm) after incubation with HeLa cells for 12h and 48h, with Hoechst 33342 (blue, λ_{ex} = 358 nm; λ_{em} = 461 nm) nuclei staining and LysoTracker (green, λ_{ex} = 530 nm; λ_{em} = 590 nm) staining acidic organelles. Merged image indicates co-localization (yellow) of NPs (Cy5), Nile Red, and lysosome inside the cells. Scale bar = 10 μm.

Table 1. Characterization data for the polymers used in this study.

Polymer	M_n / kDa	$Đ_M$
(1)	10.7[a]	1.25[a]
(4)	8.6[a]	1.20[a]
(6)	2.2[b]	1.21[b]
(1-*b*-4)(pH 4.0)[c]	18.0[a]	1.21[a]
(1-*b*-4) (pH 7.4)[c]	17.8[a]	1.14[a]
(1-*b*-4) (pH 9.2)[c]	17.3[a]	1.17[a]
(4-*b*-6) (pH 4.0)[c]	11.9[a]	1.23[a]

calculated by SEC eluting with DMF with [a)]PEG as standards; with [b)]PMMA as standards; [c)] the block copolymers were obtained from the aqueous solutions with different pH.

ASSOCIATED CONTENT

Supporting Information.

The Supporting Information available free of charge.

Data analysis and details of synthesis and characterization of initiators, polymers and

nanoparticles.

AUTHOR INFORMATION

Corresponding Author

*E-mail: jin.geng@ed.ac.uk (J.G.)

*E-mail: mark.bradley@ed.ac.uk (M.B.)

ACKNOWLEDGMENT

REFERENCES

(1)   Neumann, K.; Jain, S.; Geng, J.; Bradley, M. Nanoparticle "Switch-on" by Tetrazine

Triggering. *Chem. Comm.* **2016**, *52*, 11223–11226.

(2)   Wicki, A.; Witzigmann, D.; Balasubramanian, V.; Huwyler, J. Nanomedicine in Cancer Therapy: Challenges, Opportunities, and Clinical Applications. *J. Control. Release.* **2015**, *200*, 138–157.

(3)   Motornov, M.; Roiter, Y.; Tokarev, I.; Minko, S. Stimuli-Responsive Nanoparticles, Nanogels and Capsules for Integrated Multifunctional Intelligent Systems. *Prog. Polym. Sci.* **2010**, *35*, 174–211.

(4)   Roy, D.; Cambre, J. N.; Sumerlin, B. S. Future Perspectives and Recent Advances in Stimuli-Responsive Materials. *Prog. Polym. Sci.* **2010**, *35*, 278–301.

(5)   Glover, D.; Lipps, H. Towards Safe, Non-Viral Therapeutic Gene Expression in Humans. *Nat. Rev. Genet.* **2005**, 299–310.

(6)   Rodroguezhernandez, J.; Checot, F.; Gnanou, Y.; Lecommandoux, S. Toward "Smart" Nano-Objects by Self-Assembly of Block Copolymers in Solution. *Prog. Polym. Sci.* **2005**, *30*, 691–724.

(7)   Du, J.-Z.; Du, X.-J.; Mao, C.-Q.; Wang, J. Tailor-Made Dual pH-Sensitive Polymer– Doxorubicin Nanoparticles for Efficient Anticancer Drug Delivery. *J. Am. Chem. Soc.* **2011**, *133*, 17560–17563.

(8)   Mastrobattista, E.; van der Aa, M.; Hennink, W.; Crommelin, D. Artificial Viruses: a Nanotechnological Approach to Gene Delivery. *Nat. Rev. Drug. Discov.* **2006**, *5*, 115– 121.

(9)   Xu, X.; Yuan, H.; Chang, J.; He, B.; Gu, Z. Cooperative Hierarchical Self-Assembly of Peptide Dendrimers and Linear Polypeptides Into Nanoarchitectures Mimicking Viral Capsids. *Angew. Chem. Int. Edit.* **2012**, *124*, 3184–3187.

(10)   Pavlukhina, S.; Sukhishvili, S. Polymer Assemblies for Controlled Delivery of Bioactive Molecules From Surfaces. *Adv. Drug. Deliver. Rev.* **2011**, *63*, 822–836.

(11)   Liu, J.; Geng, J.; Liao, L.-D.; Thakor, N.; Gao, X.; Bin Liu. Conjugated Polymer Nanoparticles for Photoacoustic Vascular Imaging. *Polym. Chem.* **2014**, *5*, 2854–2862.

(12)   Dmitriev, R. I.; Borisov, S. M.; Düssmann, H.; Sun, S.; Müller, B. J.; Prehn, J.; Baklaushev, V. P.; Klimant, I.; Papkovsky, D. B. Versatile Conjugated Polymer Nanoparticles for High-Resolution O2 Imaging in Cells and 3D Tissue Models. *Acs Nano* **2015**, *9*, 5275–5288.

(13)   Iha, R. K.; Wooley, K. L.; Nystrom, A. M.; Burke, D. J.; Kade, M. J.; Hawker, C. J. Applications of Orthogonal "Click" Chemistries in the Synthesis of Functional Soft Materials. *Chem Rev* **2009**, *109*, 5620–5686.

(14)   Braunecker, W. A.; Matyjaszewski, K. Controlled/Living Radical Polymerization: Features, Developments, and Perspectives. *Prog. Polym. Sci.* **2007**, *32*, 93–146.

(15)   Blanazs, A.; Armes, S. P.; Ryan, A. J. Self-Assembled Block Copolymer Aggregates: From Micelles to Vesicles and Their Biological Applications. *Macromol. Rapid Comm.* **2009**, *30*, 267–277.

(16)   Kempe, K.; Krieg, A.; Becer, C. R.; Schubert, U. S. "Clicking" on/with Polymers : a Rapidly Expanding Field for the Straightforward Preparation of Novel Macromolecular Architectures. *Chem. Soc. Rev.* **2012**, *41*, 176–191.

(17)   De, P.; Li, M.; Gondi, S. R.; Sumerlin, B. S. Temperature-Regulated Activity of Responsive Polymer-Protein Conjugates Prepared by Grafting-From via RAFT Polymerization. *J. Am. Chem. Soc.* **2008**, *130*, 11288–11289.

(18)   Barner-Kowollik, C.; Prez, Du, F. E.; Espeel, P.; Hawker, C. J.; Junkers, T.; Schlaad, H.;

Van Camp, W. "Clicking" Polymers or Just Efficient Linking: What Is the Difference? *Angew. Chem. Int. Edit.* **2011**, *50*, 60–62.

(19) Hoyle, C. E.; Bowman, C. N. Thiol–Ene Click Chemistry. *Angew. Chem. Int. Edit.* **2010**, *49*, 1540–1573.

(20) Inglis, A. J.; Sinnwell, S.; Stenzel, M. H.; Barner-Kowollik, C. Ultrafast Click Conjugation of Macromolecular Building Blocks at Ambient Temperature. *Angew. Chem. Int. Edit.* **2009**, *48*, 2411–2414.

(21) Hansell, C. F.; Espeel, P.; Stamenović, M. M.; Barker, I. A.; Dove, A. P.; Prez, Du, F. E.; O'Reilly, R. K. Additive-Free Clicking for Polymer Functionalization and Coupling by Tetrazine–Norbornene Chemistry. *J. Am. Chem. Soc.* **2011**, *133*, 13828–13831.

(22) Ban, H.; Gavrilyuk, J.; Carlos F Barbas, I. Tyrosine Bioconjugation Through Aqueous Ene-Type Reactions: a Click-Like Reaction for Tyrosine. *J. Am. Chem. Soc.* **2010**, *132*, 1523–1525.

(23) Ban, H.; Nagano, M.; Gavrilyuk, J.; Hakamata, W.; Inokuma, T.; Carlos F Barbas, I. Facile and Stabile Linkages Through Tyrosine: Bioconjugation Strategies with the Tyrosine-Click Reaction. *Bioconjugate Chem.* **2013**, *24*, 520–532.

(24) Bauer, D. M.; Ahmed, I.; Vigovskaya, A.; Fruk, L. Clickable Tyrosine Binding Bifunctional Linkers for Preparation of DNA–Protein Conjugates. *Bioconjugate Chem.* **2013**, *24*, 1094–1101.

(25) De Bruycker, K.; Billiet, S.; Houck, H. A.; Chattopadhyay, S.; Winne, J. M.; Prez, Du, F. E. Triazolinediones as Highly Enabling Synthetic Tools. *Chem. Rev.* **2016**, *116*, 3919–3974.

(26) Hu, Q.-Y.; Allan, M.; Adamo, R.; Quinn, D.; Zhai, H.; Wu, G.; Clark, K.; Zhou, J.; Ortiz, S.; Wang, B.; *et al.* Synthesis of a Well-Defined Glycoconjugate Vaccine by a Tyrosine-Selective Conjugation Strategy. *Chem. Sci.* **2013**, *4*, 3827–3832.

(27) Vinciguerra, D.; Tran, J.; Nicolas, J. Telechelic Polymers From Reversible-Deactivation Radical Polymerization for Biomedical Applications. *Chem. Comm.* **2018**, *54*, 228–240.

(28) Liu, P.; Cai, Z.; Kang, J. W.; Boyle, A. J.; Adams, J.; Lu, Y.; Mbong, G. N. N.; Sidhu, S.; Reilly, R. M.; Winnik, M. A. Intracellular Routing in Breast Cancer Cells of Streptavidin-Conjugated Trastuzumab Fab Fragments Linked to Biotinylated Doxorubicin-Functionalized Metal Chelating Polymers. *Biomacromolecules* **2014**, *15*, 715–725.

(29) Lopalco, M.; Koini, E. N.; Cho, J. K.; Bradley, M. Catch and Release Microwave Mediated Synthesis of Cyanine Dyes. *Org. Biomol. Chem.* **2009**, *7*, 856–859.

(30) Piper, J. R.; McCaleb, G. S.; Montgomery, J. A. 10-Propargylaminopterin and Alkyl Homologs of Methotrexate as Inhibitors of Folate Metabolism. *J. Med. Med.* **1982**, 877–880.

(31) De, P.; Gondi, S. R.; Sumerlin, B. S. Folate-Conjugated Thermoresponsive Block Copolymers: Highly Efficient Conjugation and Solution Self-Assembly. *Biomacromolecules* **2008**, *9*, 1064–1070.

(32) Matyjaszewski, K. Atom Transfer Radical Polymerization. *Chem. Rev.* **2001**, *101*, 2921–2990.

(33) Gao, W.; Chan, J. M.; Farokhzad, O. C. pH-Responsive Nanoparticles for Drug Delivery. *Mol. Pharm.* **2010**, *7*, 1913–1920.

(34) Low, P. S.; Henne, W. A.; Doorneweerd, D. D. Discovery and Development of Folic-Acid-Based Receptor Targeting for Imaging and Therapy of Cancer and Inflammatory

Diseases. *Accounts Chem. Res.* **2008**, *41*, 120–129.

(35) Sudimack, J.; Lee, R. J. Targeted Drug Delivery via the Folate Receptor. *Adv. Drug. Deliver. Rev.* **2000**, *41*, 147–162.

(36) Mackiewicz, N.; Nicolas, J.; Handké, N.; Noiray, M.; Mougin, J.; Daveu, C.; Lakkireddy, H. R.; Bazile, D.; Couvreur, P. Precise Engineering of Multifunctional PEGylated Polyester Nanoparticles for Cancer Cell Targeting and Imaging. *Chem. Mater.* **2014**, *26*, 1834–1847.

(37) Sheikh Shahalom; Tony Tong; Simon Emmett, A.; Brian R Saunders. Poly(DEAEMa-Co-PEGMa): a New pH-Responsive Comb Copolymer Stabilizer for Emulsions and Dispersions. *Langmuir* **2006**, *22*, 8311–8317.

(38) and, A. S. L.; Gast, A. P.; and, V. B.; Armes, S. P. Characterizing the Structure of pH Dependent Polyelectrolyte Block Copolymer Micelles. *Macromolecules* **1999**, *32*, 4302–4310.

(39) Pocker, Y.; Green, E. Hydrolysis of D-Glucono-.Delta.-Lactone. I. General Acid-Base Catalysis, Solvent Deuterium Isotope Effects, and Transition State Characterization. *J. Am. Chem. Soc.* **1973**, *95*, 113–119.

(40) Draper, E. R.; Eden, E. G. B.; McDonald, T. O.; Adams, D. J. Spatially Resolved Multicomponent Gels. *Nat. Chem.* **2015**, *7*, 848–852.

(41) Talelli, M.; Barz, M.; Rijcken, C. J. F.; Kiessling, F.; Hennink, W. E.; Lammers, T. Core-Crosslinked Polymeric Micelles: Principles, Preparation, Biomedical Applications and Clinical Translation. *Nano Today* **2015**, *10*, 93–117.

(42) Read, E. S.; Armes, S. P. Recent Advances in Shell Cross-Linked Micelles. *Chem. Comm.* **2007**, *43*, 3021–3035.

(43) Kataoka, K.; Harada, A.; Nagasaki, Y. Block Copolymer Micelles for Drug Delivery: Design, Characterization and Biological Significance. *Adv. Drug. Deliver. Rev.* **2012**, *64*, 37–48.

(44) Geisow, M. J.; Evans, W. H. pH in the Endosome. *Exp. Cell Res.* **1984**, *150*, 36–46.

(45) Gerweck, L. E.; Seetharaman, K. Cellular pH Gradient in Tumor Versus Normal Tissue: Potential Exploitation for the Treatment of Cancer. *Cancer Res.* **1996**, *56*, 1194–1198.

(46) Wang, Y.; Zhou, K.; Huang, G.; Hensley, C.; Huang, X.; Ma, X.; Zhao, T.; Sumer, B. D.; DeBerardinis, R. J.; Gao, J. A Nanoparticle-Based Strategy for the Imaging of a Broad Range of Tumours by Nonlinear Amplification of Microenvironment Signals. *Nat. Mater.* **2014**, *13*, 204–212.

(47) Ghanbarzadeh, S.; Arami, S.; Pourmoazzen, Z.; Ghasemian-Yadegari, J.; Khorrami, A. Plasma Stable, pH-Sensitive Fusogenic Polymer-Modified Liposomes: a Promising Carrier for Mitoxantrone. *J. Biomater. Appl.* **2013**, *29*, 81–92.

(48) Liu, J.; Huang, Y.; Kumar, A.; Tan, A.; Jin, S.; Mozhi, A.; Liang, X.-J. pH-Sensitive Nano-Systems for Drug Delivery in Cancer Therapy. *Biotechnol. Adv.* **2014**, *32*, 693–710.

1
2
3
4
5
6
7
8
9
10
11
12
13
14
15
16
17
18
19
20
21
22
23
24
25
26
27
28
29
30
31
32
33
34
35
36
37
38
39
40
41
42
43
44
45
46
47
48
49
50
51
52
53
54
55
56
57
58
59
60

Table of Contents Graphic

Polymer A

Polymer B

+

PTAD-phenol
reaction

aqueous solution
room temperature

Multi-functional nanopartilce

Block copolymer

Imaging

OH

Targeting

29